PHILOSOPHICAL TRANSACTIONS OF THE ROYAL SOCIETY A MATHEMATICAL, PHYSICAL & ENGINEERING SCIENCES

Modern Design of Belt Conveyors in the Context of Stability Boundaries and Chaos

A. Harrison

Phil. Trans. R. Soc. Lond. A 1992 **338**, 491-502
doi: 10.1098/rsta.1992.0016

Modern design of belt conveyors in the context of stability boundaries and chaos

By A. Harrison

Winders, Barlow and Morrison, Englewood, Colorado 80112, U.S.A. and Department of Engineering, Colorado School of Mines, Golden, Colorado, U.S.A.

Belt conveying of bulk materials has evolved to the point where the demands of the modern mine to increase capacity is limited by the ability of engineers to design dynamically stable conveyors. Belt speed and width are two parameters that may be varied in the design to provide the required material flow rate. For certain values of belt speed, width and tension, unstable transverse belt vibration has been observed. Large-amplitude vibration may be so severe that the life of the supporting idler bearings is reduced significantly due to dynamic loads. Monitoring idlers for bearing failure in modern conveyors with lengths up to 20 km is practically difficult since there may be as many as 20000 idler sets. Chaotic transverse belt vibrations occur for certain levels of excitation, further complicating the prediction of bearing life. Before conveyor installation, an estimate of the stability boundaries for resonance-free operation is an essential precursor to failure-free conveyor operation. Nonlinear resonance phenomena such as belt flap is sensitive to initial conditions. The effects of chaotic vibrations on the predictability of design stability is reviewed using some examples of forced vibrations.

1. Introduction

Current conveyor design practice outlined in the International Standard ISO5048 (1979) is based on belt sag and rolling friction, and both need to be minimized to minimize belt power consumption. In achieving this goal the support structure of the carry and return-side belting is designed to maintain belt sag below 3% by the appropriate use of belt pre-tensioning. In this respect, the conveyor design may be optimum for steady-state operation but the belt will usually exhibit severe transverse vibrations at some location along its length due to idler support excitation.

Design parameters of modern conveyors vary greatly and depend on the application. By way of background, a typical belt conveyor has a length of 1600 m, moves at a velocity of 3.5 m s^{-1}, has a belt width of up to 2 m, conveys mine product up and down gradients as high as 16% with a material flow rate of up to 3000 t h^{-1} and consumes power at amounts in excess of 3 MW. Larger systems do exist where tonnages of the order of 10000 t h^{-1} are conveyed and where the belt length exceeds 20000 m.

There are two distinctive dynamic effects in modern conveyor belt design that are governed by nonlinear processes, namely transverse belt vibrations and longitudinal wave motion induced in the belt on starting and stopping.

Phil. Trans. R. Soc. Lond. A (1992) **338**, 491–502
Printed in Great Britain

There is a large literature on longitudinal or elastic wave propagation in belts. The belt's dynamic elastic properties on starting and stopping can result in unstable behaviour of both belt sag and drive motor power. Funke (1974) and Harrison (1981) modelled transient stresses in conveyor belts on starting and stopping using a wave model. The development of finite element models by Nordell & Ciozda (1984) verified the wave approach of earlier researchers, whereas the numerical stability of finite difference methods was researched by Morrison (1988). Although this aspect of modern conveyor design is not the thrust of this paper, variation in belt tensions during a transient phase will influence the stability of transverse vibrations on starting or stopping but this effect will not govern the failure rate of idlers.

A more important aspect of modern conveyor belt design is the analysis of the dynamic stability of moving, unsupported belting under an axial tension. Harrison (1979) investigated the transverse flexural vibrations of flat and troughed steel cord reinforced belting using non-contact variable reluctance magnetic transducers. These transducers (U.S. Patent 4439731) permitted the measurement of the vibration frequencies of the flapping belt as it moved on its roller supports. Deflections of the order of 150 mm are observed at resonance and the ease in which resonances are excited is a direct consequence of the small amounts of internal and external damping, leading to a high mechanical Q near 100. Measurements indicate the presence of nonlinear processes that are usually unstable and often chaotic.

Prediction of the transverse vibration frequencies of a running belt under axial tension involves the development of a mechanical model of the problem. Plate mechanics have been used by Harrison (1983*a*, *b*) to describe the problem including its viscoelastic boundary conditions. Although one may predict with good accuracy the flexural frequencies of the vibrating belt, the boundaries for flexural stability are more difficult to analyse because the problem itself is sensitive to initial conditions. For example, the belt's mass may vary slightly, belt surface friction is not constant, and idler rotation frequency will shift as fine material adheres to the idler during conveyor operation.

Phase plane portraits of the transverse vibration of unsupported belting have been used with success to show the existence of strange attractor motion and period doubling, as reported by Harrison (1990). Unstable and chaotic effects might be expected with flapping belts since the deflections become large and lift-off of the belt from its idler support will extinguish the resonant cavity. Idlers are often manufactured with a small amount of eccentricity and so form a basic source of rotational forcing excitation for the belt.

Conveyor belt system design will be reviewed in the context of stability boundaries and chaos of the transverse vibration problem. The prediction of stability boundaries is needed early in the design of the conveyor to allow estimating engineers to take into account the influence of these dynamic factors in the project's costing.

2. Modern design philosophy

The mining industry is continually trying to reduce handling and conveying costs. This philosophy has led conveyor system manufacturers and design engineers to develop designs that use wider belts, resulting in considerable structural cost penalty as pointed out by Roberts *et al.* (1981). To move large volumes of bulk materials, the alternative of narrow fast belts proposed by Harrison & Roberts (1983) requires the application of dynamic analysis to the design. An emphasis on the concept of design

PHILOSOPHICAL TRANSACTIONS OF THE ROYAL SOCIETY A MATHEMATICAL, PHYSICAL & ENGINEERING SCIENCES

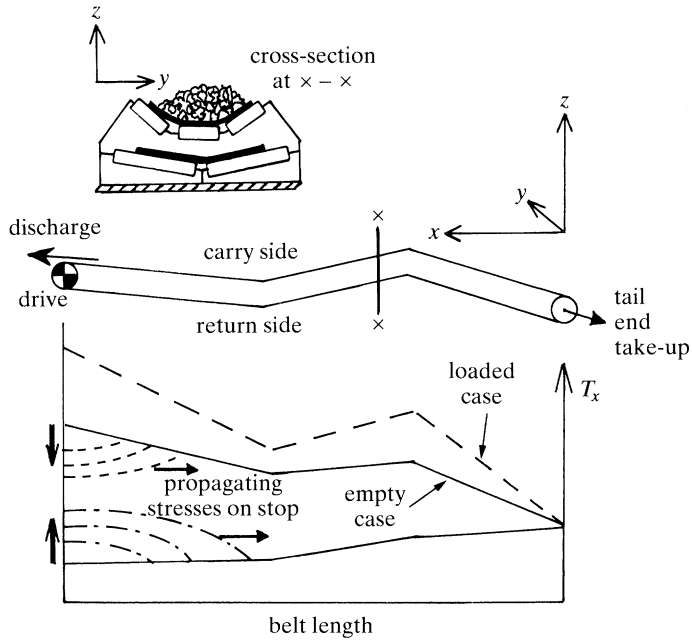

Figure 1. Conveyor belt tensions and wave dynamics.

for reliability is applicable in modern conveyor technology. The effect of parametric variations in boundary conditions on the stability of the design is therefore directly applicable in design reliability.

Narrow high-speed belts are 'less prone' to transverse vibration since belt flap frequencies are usually beyond idler excitation frequencies. Flapping belt can reach large amplitudes resulting in lift off and dynamic impact that will overload idler support rollers, causing premature failure of idler bearings. The speed and width of the belt is selected to ensure that the design capacity of the system is achieved.

Before discussing the dynamics of a transversely vibrating conveyor belt, one need to supply some background to conveyor design. Figure 1 illustrates a side elevation schematic of a typical long conveyor, including a cross-section of the loaded belt and the running tensions around the system for loaded and unloaded states. A belt's tension distribution along its length is due to combinations of gravity acting on the system mass and rolling friction. The axial tension in the belt is one of the more important parameters governing resonance location. On starting or stopping, belt tensions vary and so resonances may appear and disappear during this phase of operation. Figure 1 may be used to illustrate the changing belt tensions on starting or stopping, and in this case, for the empty belt condition. Tension changes propagate at the speed of sound in the belt as described by Harrison (1991).

The transverse modes of vibration of a conveyor belt, at any cross-section × – × in figure 1, needs to be established to carry out stability studies.

Flexural vibration of the unsupported return strand of belting is of greatest interest in the design of the modern high-speed conveyor belt because of the possibility of large amplitude resonances. Figure 2 shows an example of some commonly observed flexural shapes of a transversely vibrating belt.

The partial differential equation of motion for the moving belt is described using the usual notation (Harrison 1983). In the notation, w describes the belt deflection

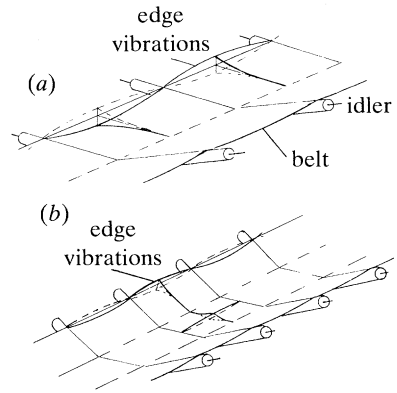

Figure 2. Some typical flexural shapes of vibrating belts. (*a*) V-return, (*b*) three-roll trough.

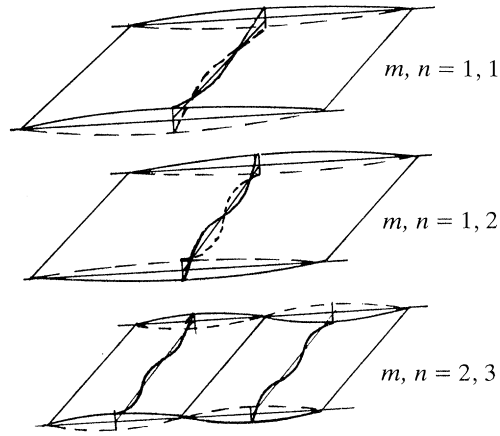

Figure 3. Vibrations that become unstable in flat belts.

in the vertical z axis, x defines the axis in the direction of belt travel and y represents the axis across the belting. The partial differential equation describing the transverse flexural motion of the belt is

$$D_x\frac{\partial^4 w}{\partial x^4}+2D_{xy}\frac{\partial^4 w}{\partial x^2\,\partial y^2}+D_y\frac{\partial^4 w}{\partial y^4}=-M_{\mathrm{B}}(\ddot{w}+\phi),\quad 2v\frac{\partial^2 w}{\partial x\,\partial t}+E^2\frac{\partial^2 w}{\partial x^2}+K\dot{w}=\phi, \tag{2.1}$$

where D represents a flexural rigidity, M_{B} is the belt mass per unit length, v is the belt speed, K is the damping, $E^2=(v^2-T_x(y)/M_{\mathrm{B}})$ and $T_x(y)$ is the tension distribution across the belt at a location x along the profile. In reality, $T_x(y)$ is non-uniform and for analysis of the problem it is assumed that the belt tension has an average value T_x.

Built-in manufacturing anomalies affect the load sharing of the axial reinforcing members inside the rubber belt, and these anomalies are the origin of $T_x(y)$. This variable affects the transverse vibration frequency and so contributes to the uncertainty in the boundary conditions for resonance prediction. Given the above constraints, the natural frequency plate modes (m, n) for each vibrating belt span moving at speed v is determined by

$$f_{mn}(v)=f_{mn}(0)[1-v^2/c^2], \tag{2.2}$$

where $f_{mn}(0)$ is the zero speed natural plate frequency, and c is determined using

$$c^2 = [D_x g_{mn}^2/(M_B(m\pi a)^2)] - E^2, \tag{2.3}$$

$$f_{mn}(0) = mc/2a, \tag{2.4}$$

with m the mode of vibration along x (the axial belt direction), n is the mode across the belt and a is the idler spacing. Values of the non-dimensional frequency parameter g_{mn} are governed by the plate aspect ratio (length-to-width) as discussed by Harrison (1986). Figure 3 shows a selection of some commonly observed mode shapes for a vibrating span of a flat belt. These modes easily become unstable.

In keeping with the aim of this paper to provide engineers with a design methodology that results in a dynamically stable conveyor, the range in the frequency of belt vibration needs to be established. The frequency of a particular mode of belt vibration should first be calculated and then the system design needs to ensure that this frequency is located above the idler excitation frequency by appropriate selection of the belt speed, idler spacing, idler diameter and belt tension. With an idler diameter d, the idler excitation frequency is simply

$$f_i = v/\pi d. \tag{2.5}$$

Another approach that is often successful in maintaining a high belt frequency is to design a conveyor with a high aspect ratio. A narrow (0.9 m), longitudinally stiff belt will have a natural frequency above a wider, more flexible belt. This approach will ensure that g_{mn} is large which in turn will result in a high belt frequency. Belt bending stiffness also enters into the equation of motion and therefore a stiff belt (D large) will have a higher frequency than one with a small value of D. Idler spacing d is one other variable that may be used very effectively by the design engineer. If unstable transverse vibrations occur the idler spacing may be reduced to increase f_{mn} but then the number of idler sets increase and so does the system cost.

Clearly, those parameters that most affect the predictability of the belt's resonance frequency are localized belt mass variations, localized variations in g resulting from changes to the plate aspect ratio as the belt mistracks, variations in belt tension $T_x(y)$ due to nonlinear viscoelastic temperature effects and local variations in belt bending stiffness. Each of these parameters have an influence on the stability window, which may be defined as

$$(f_{mn}(v) - C_1) < f_i < (f_{mn}(v) - C_2), \tag{2.6}$$

where C_1 and C_2 are the lower and upper bounds of the belt's natural frequency as discussed above. Belt tension $T_x(y)$ (and its average value T_x) still remain the governing restoring forces in the belt and so will affect the natural frequencies of the belt to the greatest extent.

However, the variability in natural modal frequency leads to instabilities and chaotic tendencies in a vibrating belt. The frequencies themselves are totally determinable for any given set of conditions that can be defined. When nonlinear interactions begin to dominate the motion through large-amplitude deflections or axial forcing due to vibration of adjoining spans, the design contains resonances that are not predictable and are damaging to the supporting structure.

3. Large amplitude vibrations and chaos

In most conveyor belt installations, small-amplitude vibrations (less than 10 mm) are always present and are usually the result of irregularities in the conveyor belting and structure. Near-resonant spans behave very differently. Once a boundary

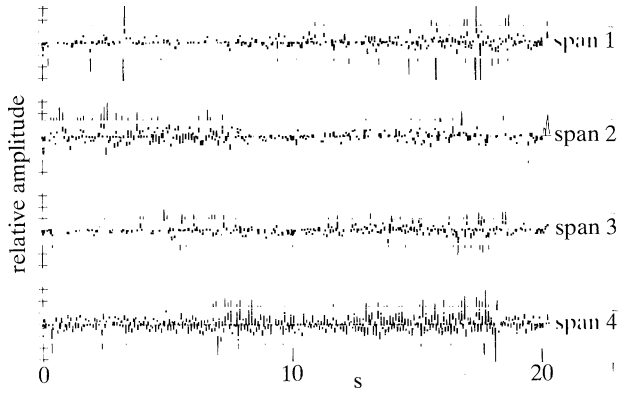

Figure 4. The unstable vibrations of four spans of flat belting.

condition such as load or temperature changes in the system, unknown resonances may be excited depending on how close the span of belting is to resonance, according to (2.6). Forced vibrations result in large amplitudes of vibration (greater than 150 mm). The uncontrolled 'whipping' of the belt under this driving condition is irregular and prone to drop-out similar to that observed in systems that exhibit hardening effects.

The speed of sound in conveyor belt material is determined using (2.3). When belt speed and stiffness are neglected ($v \ll c, D \ll T_x$), the tension has a dominant influence on belt model frequency. Since a belt supported on multiple idlers can be represented by a system of connected plates with boundaries at the idler support, it is possible that resonance effects in one particular span will influence adjoining spans. In this case, span frequency will be perturbed by fluctuating axial tensions which have a maximum value on two occasions during one flexural cycle. Replacing E^2 in (2.1) by a time-dependent variation in tension leads to

$$(T_x + \delta T_x \cos 2\omega_m t)w'' - KM_B \dot{w} - M_B \ddot{w} = 0 \quad (0 < \delta < 1). \tag{3.1}$$

Experimental data are used to provide evidence of the nature of the flexural cascades that occur in resonant belt conveyors. Figure 4 shows the coincident time records of four flat belt spans showing unstable oscillations.

The example in figure 4 shows data recorded from a steel cord reinforced belt type SR2500 used in a slope conveyor application at a coal mine. The belt was 1.15 m wide with a speed of 3.4 m s^{-1} and a support spacing of 2.5 m. The belt has a flap frequency of 8.5 Hz $\pm$ 0.53 Hz. Amplitudes of about 10 cm were recorded. It is noteworthy that over the 20 s interval, each span has its own unique amplitude and phase. Expanding one portion of the data to record a 2 s interval reveals the nearly sinusoidal nature of the vibrations except for parts of the waveform that exhibit dropout behaviour. Figure 5 shows the 2 s interval of vibration of the four spans of belting, including the relative flexural phases of the vibration.

The upper portion of figure 6 shows the instantaneous flexural positions of the 4 spans of belting at time intervals equivalent to $\frac{1}{4}$ of the vibration frequency. The lower portion of the figure reconstructs the flexural model in the time domain. One notes the similarity of the hypothetical waveforms to those recorded from an actual belt in figure 5.

Interpretation of the vibration record in figure 5 is facilitated by figure 6. Spans 1 and 2 are vibrating in a flexural cascade mode where the slope at the idler support

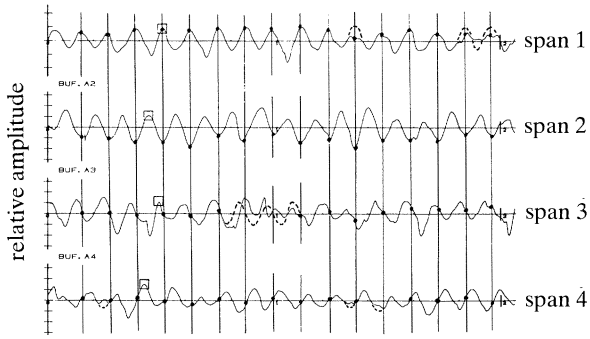

Figure 5. A two second time record for data in figure 4.

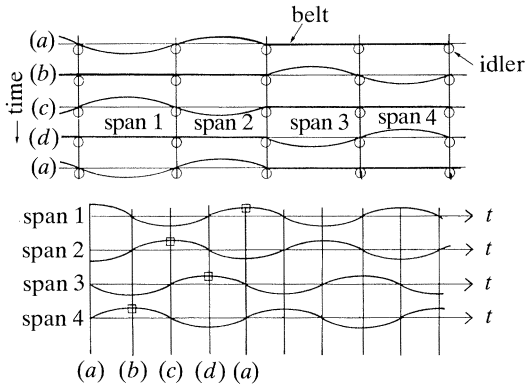

Figure 6. Reconstruction of the vibration phases in figure 5.

is preserved. This is also the case for spans 3 and 4. However, at the idler support between span 2 and 3 the belting's slope is not preserved and so a tension fluctuation in the 1–2 and 3–4 span forces the conservation of belt tension in the 2–3 span. Obviously this system is very unstable and readily dependent on initial conditions such as belt stiffness, mass and the shape of $T_x(y)$.

Observing that the motion of each span is essentially sinusoidal, the deflection w in (3.1) may be cast in the form

$$w(x,t) = A_0 \sin kx\, \theta(t) \tag{3.2}$$

and substitution into (3.1), reveals the well-known Mathieu equations

$$M_B \ddot{\theta} + (K^2 T_x + K^2 \delta T_x \cos 2\omega_m t)\,\theta + K M_B \dot{\theta} = 0, \tag{3.3}$$

where the coefficient of θ varies periodically at twice the belt frequency in the axial direction. Equation (3.3) may also be shown to be equivalent to a forced Duffing equation, as discussed by Jordan *et al.* (1987),

$$\ddot{\theta} + K\dot{\theta} + (\alpha\theta + \beta\theta^3) = F_0 \cos \Omega t. \tag{3.4}$$

Chaotic and periodic doubling solutions can be obtained from this function due to the presence of a nonlinear term in the stiffness, as the forcing frequency is varied. At large amplitudes, the motion is expected to produce unstable behaviour.

In figures 4 and 5, belt vibrations were self excited by an eccentric idler support, rotating at a frequency near that of the natural frequency. Amplitude stability was

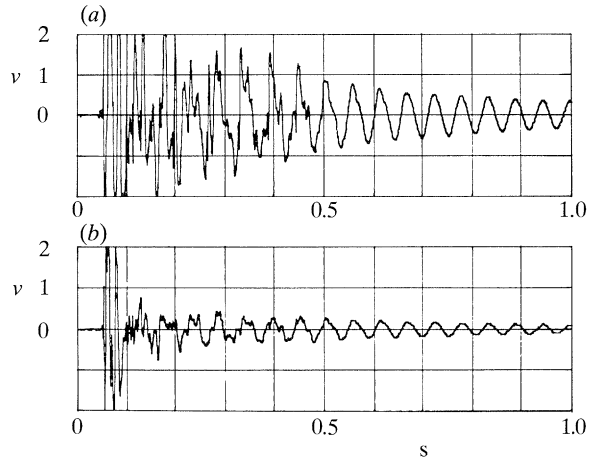

Figure 7. Large-amplitude vibrations and transient chaos.

governed by initial conditions and also by the degree of periodic forcing at twice the belt flap frequency. There are at least four distinct types of flexural interactions identified by Harrison (1990) and these are similar to that of figure 6. The type shown in figure 6 is most commonly observed.

Chaotic outcomes may be demonstrated when the amplitudes of vibration become large. Not only does the stiffness term cause nonlinear 'jump' processes resulting in drop-out behaviour and resonance collapse, it will also drive the vibrations to the point of period doubling through a bifurcation when the forcing frequency is near the natural model frequency. At large amplitudes of vibration, belt lift-off occurs and this creates severe instabilities.

4. Forced vibrations and chaotic instability

Two methods have been used to generate large amplitude vibrations in moving and stationary belts, namely hammer impact excitation and non-contact shaker excitation. Impact excitation using a large hammer is an effective method of exciting a tensioned belt to observe the evolution of the motion.

Figure 7 shows the response of a V-return section of belting following hammer impact. During the initial 0.5 s of the vibration the motion is highly aperiodic, but eventually the motion stabilizes to a periodic motion with a point attractor. The frequency of vibration of the 20 Hz sinusoid represents the small-amplitude response of the belt and is free from nonlinearities. In figure 7, the upper trace represents the response of the right-hand side of the V-return whereas the lower trace represents the left-hand portion of the V-return as in figure 2.

During the chaotic phase, there is strong evidence that two attractors are present at the extremities of the response and these are due to span–span interactions between competing tension oscillations. The fact that both waveforms in figure 7 are in-phase for small amplitude oscillations is due to an induced moment acting at the V-return bend line. Steady state oscillation at a fixed frequency occurred when the amplitude of the vibration decayed to a peak to peak value of 40 mm. In this case, the belting has similar dimensions and physical characteristics to the flat belt described earlier.

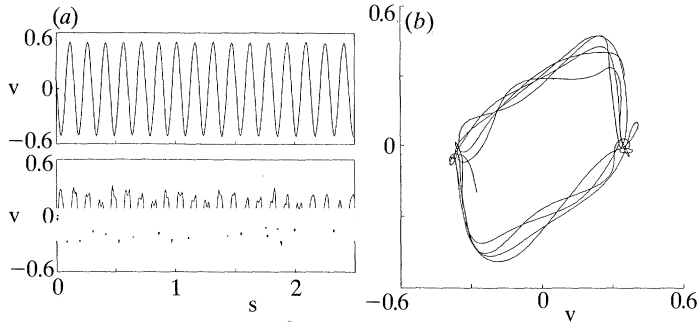

Figure 8. (*a*) Forcing current and transverse belt response just before resonance (upper and lower time traces respectively) and (*b*) the phase plane response of the belt time record.

Forced transverse vibration of a steel cord reinforced belt has also been achieved using a non-contact electromagnet shaker. Weighing 70 kg, the shaker was placed beneath the midspan of a belt with similar physical characteristics to the belt described earlier. The shaker was designed to impart a small periodic pulling force on the steel reinforced belt from a distance of 150 mm.

Advantages of this experiment in determining boundaries of stability are numerous, including the ability to scan the shaker's drive current from 0–40 Hz at power levels of 1 kW. An experiment of this type provides the resonance response curve, permits the calculation of Q and damping and allows all tests to be made in a non-contact manner while the belt is in operation. In addition, the stability of each span can be monitored to determine the influence of the above governing parameters (width, mass per unit length, $T_x(y)$ and speed) on the frequencies of adjoining spans.

Figure 8 shows the results of a shaker test on a steel cord belt. The upper signal trace represents the shaker coil current as a function of time, and the lower signal trace is the belt's vibratory response. The belt's natural frequency was 9.0 Hz. In this experiment, the forcing current in the coil of the shaker would vary about zero, at a frequency of about 3.5 Hz, giving an actual field pulling force at 7 Hz. At 7 Hz excitation, period doubling occurred, as shown in the response signals, where one observes a bifurcation at the extremities of the belt's deflection. Phase plane representation of this vibration near 9 Hz clearly shows the two strange attractor regions.

Further insight into the mechanics of the problem may be gleaned as the frequency of excitation increases through the natural resonance point. Large amplitude deflections begin to occur at approximately 8.75 Hz. The deflections build up to a peak of about ± 100 mm at 8.9 Hz, but just beyond this forcing frequency, the response drops dramatically. A 'hole' in the resonance response curve has the hallmarks of nonlinearity that are often associated with lift-off or boundary condition modification. In this case belt lift-off resulted in a momentary collapse of all vibrations in that given span, but adjoining spans would begin to flex as described earlier. Figure 9 (left side) shows the hole following resonance in the fast Fourier transform 'up' scan.

During the down frequency scan from 20 Hz to 0 Hz, one observes the hole just below 9 Hz. Large deflections of the belt have caused lift-off and a subsequent uncoupling of the idler boundary support, resulting in this response.

Poincaré map representation of the forced motion in the above example is shown in figure 10. Not shown in this one map is a shift in structure of the map as the

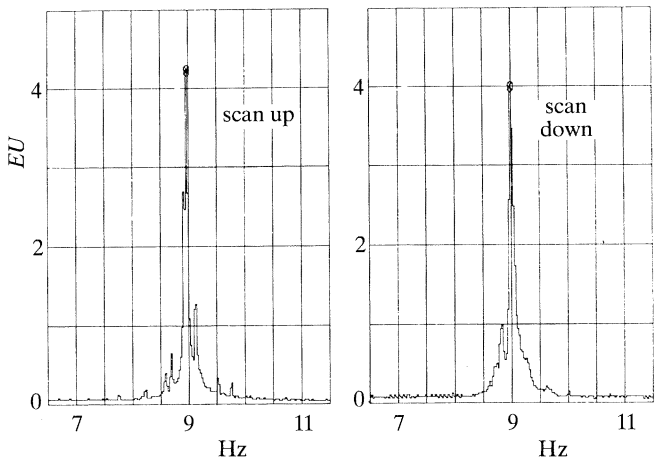

Figure 9. Forced resonance curves for an 'up' and 'down' scan showing the drop-out phenomena either side of resonance.

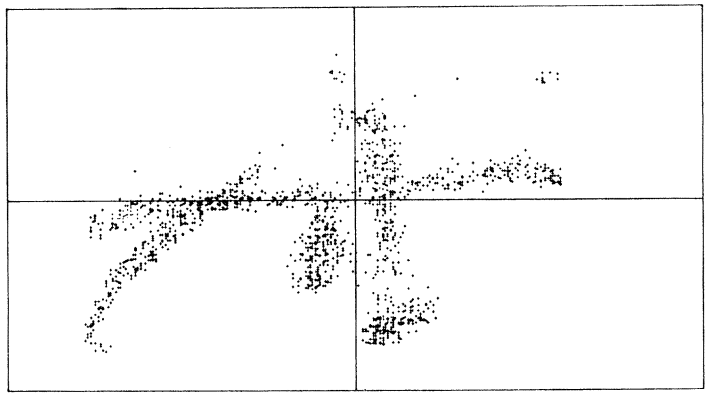

Figure 10. Poincaré map of a 20 s forced vibration.

belt is allowed to continually vibrate under shaker excitation near the resonant $(m, n) = 1, 1$ mode. Variations in the sub-harmonic content over time have been viewed as moving structure in the Poincaré map. There is some evidence that the vibration contains fractal structure but damping in this case is very small and there are insufficient points in the map record to fully observe damping influences. The period of vibration near resonance is also difficult to quantify in this example.

5. Design considerations

There is sufficient evidence that transverse belt vibration is, on the one hand, damaging to a design and on the other, controllable by proper selection of components. Figure 11 shows the basic design variations that may be implemented with regard to idler spacing. The correct positioning of the idlers is perhaps the single most practical method of obtaining a resonance-free belt.

Figure 11 has been included in this paper to show the strategy behind the redesign of a conveyor structure to remove transverse belt vibrations. Usually the reduction of resonances at a design stage or for a working conveyor is a difficult task to achieve

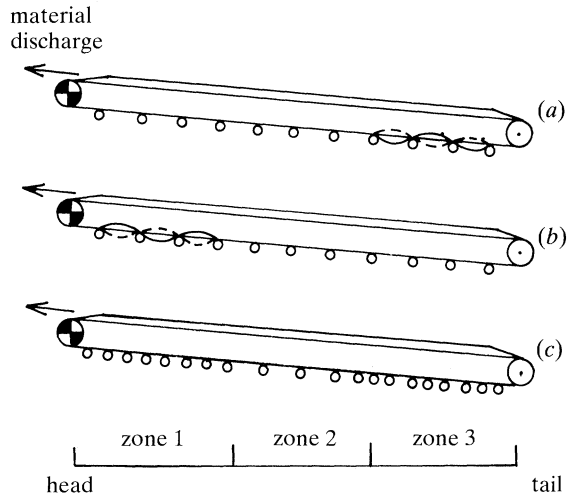

Figure 11. Concept of resonance removal by structural redesign. (*a*) Resonance at pre-tension 1, (*b*) resonances at pre-tension 2, (*c*) design for no resonances.

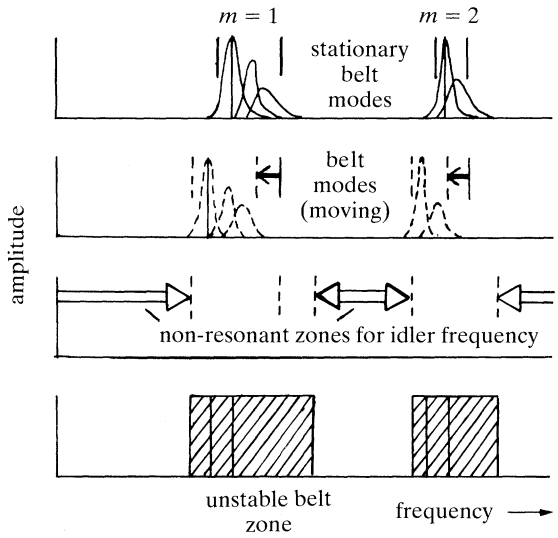

Figure 12. Specifying the boundaries of instability and chaos.

because the conveyor structure is modular. Usually idlers are located at a vertical beam support position and these are governed by steel strength for a certain unsupported length of total conveyor. Belt sag is also kept to a maximum of about 3% and these considerations form the basis for cost estimates during design.

Conveyors may be retro-fitted with additional idlers to remove transverse vibrations, but due to the mechanical constraints imposed by the structure, this approach is costly and usually means that additional structure is required to be added to the existing support. Figure 12 illustrates the design boundaries for belt stability through idler excitation sources.

The common modal frequencies for the belt for a given tension at a given temperature (upper trace) are modified for belt speed (second trace). The third trace

includes increases in belt frequency due to parametric variations in belt mass or stiffness, and the final record shows the unstable regions. Idler diameters should be selected so that operation is in the stable zones (figure 12) and preferably below the first mode's zone of instability. In the design solution space one can use the following guidelines:

(i) calculate the belt natural frequency and excitation frequencies;
(ii) determine a stability boundary based on parameter variations;
(iii) determine the location of zones of resonances along a belt;
(iv) modify idlers configuration or change take-up mass to remove resonances.

6. Concluding comments

Design of mechanical belt conveyors requires the application of dynamic analysis to predict locations of transverse vibrations. The equations defining the motion of a moving belt have been determined. Apart from irregularities in the various parameters that govern the vibration, the system is essentially deterministic until large amplitudes of vibration appear. Large-amplitude resonances result in period doubling and chaotic motion and these effects have been measured and the techniques for measuring these chaotic vibrations have been described.

Of great interest to design engineers is the boundary of stability of a given design. The paper has discussed by way of example the many and various limits that need defining to submit a dynamically stable design. A number of options have been described that apply the new insights of chaos theory to this nonlinear forcing problem and experiments have suggested that the rotational frequency of idlers needs to be about 2 Hz below the highest belt frequency, to prevent large amplitude vibrations that whip chaotically and cause idler destruction.

References

Funke, H. 1973 Zum Dynamischen Verhalten von Forderbandanlagen beim Anfahren und stillsitzen. Dissertation, TU Hannover, Germany.

Harrison, A. 1979 New developments on conveyor belt monitoring. *Mach. Prod. Engng* **32**, 17.

Harrison, A. 1983*a* Criteria for minimizing transient stresses in conveyor belts. *Mech. Engng Trans.* **8**, 129–134.

Harrison, A. 1983*b* Flexural behaviour of tensioned conveyor belts. *Mech. Eng. Trans.* **8**, 124–128.

Harrison, A. & Roberts, A. W. 1983 Technical requirements for operating conveyor belts at high speed. In *Proc. Int. Conf. on Bulk material storage handling and transport*, vol. 7, pp. 84–89. IEAust.

Harrison, A. 1986 Determination of the natural frequencies of transverse vibration of conveyor belts with orthotrophic properties. *J. Sound Vib.* **110**, 483–493.

Harrison, A. 1990 Dynamic instabilities and chaos in running belts and their cleaning devices. In *Proc. EPRI workshop on chaos*. San Francisco.

Harrison, A. 1991 Dynamic sag instabilities in long underground belt conveyors. In *Proc. Int. Mech. Eng. Congr.*, pp. 24–31. Sydney.

Jordan, D. W. & Smith, P. 1982 *Nonlinear ordinary differential equations*. Oxford: Clarendon Press.

Morrison, W. R. B. 1988 Computer graphics techniques for visualizing belt stress waves. *Bulk Solids Handlings* **8**, 221–227.

Nordell, L. K. & Ciozda, Z. P. 1984 Transient Salt Stresses during starting and stopping & elastic response simulated by finite element methods. *Bulk Solids Handling Int. J.* **4**, 93–98.

Roberts, A. W., Hayes, J. W. & Scott, O. J. 1981 Optimal design of Continuous Conveyors. *Bulk Solids Handling Int. J.* **1**, 255–264.

PHILOSOPHICAL TRANSACTIONS OF THE ROYAL SOCIETY A MATHEMATICAL, PHYSICAL & ENGINEERING SCIENCES